University of Bath

Voltage-Activated Ca^{2+} Channels in Rat Renal Afferent and Efferent Myocytes: No Evidence for the T-Type Ca^{2+} Current

Sergey Smirnov[1], Kathy Loutzenhiser[2], Rodger Loutzenhiser[2]

[1]Department of Pharmacy and Pharmacology,
University of Bath,
Claverton Down, Bath, BA2 7AY,
England.

[2] Smooth Muscle Research Group,
University of Calgary Faculty of Medicine,
3330 Hospital Drive, N.W.
Calgary, Alberta, T2N 4N1,
Canada.

Address Correspondence to:

Dr. Sergey Smirnov
Department of Pharmacy and Pharmacology,
University of Bath,
Claverton Down, Bath, BA2 7AY,
England.

phone: 0044 1225 384471
Fax: 0044 1225 386114
email: S.V.Smirnov@bath.ac.uk

Key Words: Renal Microcirculation, L-type Ca^{2+} Channels, T-type Ca^{2+} Channels, Tail Artery, Patch Clamp, Afferent Arteriole

Abstract:

Aims: Based on indirect methods, it has been suggested that both L- and T-type Ca^{2+} channels mediate signalling in the renal afferent arteriole and that T-type Ca channels are involved in signalling in the efferent arteriole. However, Ca^{2+} currents have never been studied in these two vessels. Our study was initiated to directly determine the type of Ca^{2+} channels in these vessels for the first time, using patch clamp.

Methods and Results: Native myocytes were obtained from individually isolated rat renal afferent and efferent arterioles and from rat tail arteries (TA). TA myocytes, which possess both L- and T-type Ca^{2+} currents, served as a positive control. Inward Ca^{2+} and Ba^{2+} currents (I_{Ca} and I_{Ba}) were measured in 1.5 mmol/L Ca^{2+} and 10 mmol/L Ba^{2+}, respectively, using the whole-cell configuration. By exploiting known differences in activation and inactivation characteristics and differing sensitivities to nifedipine and kurtoxin, the presence of both L- and T-type Ca^{2+} channels in TA myocytes were readily demonstrated. Afferent arteriolar myocytes exhibited relatively large I_{Ca} densities (-2.0±0.2 pA/pF) in physiologic Ca and the I_{Ba} was 3.6 fold greater. These currents were blocked by nifedipine, but not by kurtoxin and did not exhibit the activation and inactivation characteristics of T-type Ca channels. Efferent arteriolar myocytes did not exhibit a discernable voltage-activated I_{Ca} in physiologic Ca^{2+}.

Conclusions: Our findings support the physiologic role of L-type Ca^{2+} channels in the afferent, but not efferent, arteriole, but do not support the premise that functional T-type Ca^{2+} channels are present in either vessel.

1. Introduction

The renal afferent and efferent arterioles regulate the inflow and outflow resistances of the glomerulus and thereby regulate the pressure within the intervening glomerular capillaries (P_{GC}). Afferent arteriolar constriction reduces P_{GC} and, for example, prevents the transmission of systemic hypertension to the glomerulus.[1] A selective efferent vasoconstriction increases P_{GC} and is essential in preserving glomerular filtration rate (GFR) when renal perfusion is compromised.[2] Considering their differing roles and the physiologic need for independent regulation, it is not surprising that these two vessels have quite distinct regulatory mechanisms. A key difference involves the types of Ca^{2+} entry mechanisms present in each vessel.

Early studies examining the effects of Ca^{2+} channel blocking agents on renal hemodynamics suggested that such agents act selectively on pre-glomerular resistance, increasing P_{GC} and GFR.[3] This premise was confirmed as diverse approaches, developed to directly assess the effects of these agents on the renal microcirculation, demonstrated a preferential dilation of the afferent arteriole, and no effect on the efferent arteriole.[4,5] Indeed, the efferent arteriole appears to be unique, in that not only is this vessel insensitive to L-type Ca^{2+} blockers, but, with rare exceptions,[6,7] depolarization does not cause vasoconstriction or Ca^{2+} entry.[8-10] Similarly, hyperpolarization, which attenuates afferent arteriolar vasoconstriction, presumably by reducing the activities of voltage-activated Ca^{2+} channels, has no discernable effect on the efferent arteriole.[11]

Molecular approaches confirmed that L-type Ca^{2+} channel protein is preferentially expressed in the afferent arteriole,[12] but also suggested that additional species of voltage-activated Ca^{2+}

channels, including T- and N-type Ca^{2+} channels, might be expressed in the both vessel types.[12-14] With the advent of pharmacologic agents capable of blocking such channels, it was subsequently shown that T/L-type channel blockers (e.g. mibefradil, efonidipine) reverse agonist-induced vasoconstriction of both afferent and efferent arterioles in contrast to dihydropyridines, which dilate only the afferent arteriole (reviewed in[13]). Such observations have led to a prevailing view that both L- and T-type Ca^{2+} channels mediate signalling in the afferent arteriole and that T-type Ca^{2+} channels play an important role in the efferent arteriole. Nevertheless a number of facts are inconsistent with this premise. These include the lack of effect of depolarization on the efferent arteriole,[8-10] the ability of L-type selective dihydropyridines to fully block responses of the afferent arteriole[13] and the low availability of T-type Ca^{2+} channels at physiologic membrane potentials of the unstimulated afferent and efferent arteriole *in situ*t (-40 to -45 mV[15]). In this regard, it is important to note that although these agents do block T-type Ca^{2+} channels they all have other actions that can affect vascular responses.

Do T-type Ca^{2+} channels actually play an important role in the renal microcirculation or are the actions of these pharmacologic agents due to other reported effects? These questions are critical in regard to our understanding of the control of the renal circulation and have important clinical implications. For example, it has been suggested that because T-type Ca^{2+} channel blockers reverse efferent vasoconstriction, these agents are renal protective as compared to L-type Ca^{2+} blockers which by increasing P_{GC} promote hypertensive injury.[14] These considerations point to importance of studies that directly evaluate the voltage-activated Ca^{2+} channels that are present in the renal afferent and efferent arterioles using patch clamp. To our knowledge the present study is the first to do so using single myocytes freshly dispersed from individually isolated afferent and efferent arterioles.

2. Methods

All procedures complied with University of Calgary Animal Ethics and Canadian Council on Animal Care regulations and conformed with *the Guide for the Care and Use of Laboratory Animals* published by the US National Institutes of Health (NIH Publication, 8th Edition, 2011).

The characteristics of the Ca^{2+} channels present in native renal afferent (AA) and efferent (EA) arteriolar myocytes were evaluated using the whole-cell patch-clamp at room temperature (23ºC). Individual renal arterioles were isolated from the renal cortex (excluding the juxtamedullary area) of normal male Sprague–Dawley rat kidneys using the gel-perfusion technique.[8] Tissue was harvested under deep halothane anaesthesia (1.5-2% flow rate, assessed by the absence of paw withdrawal reflex) and animals were euthanized by exsanguination. Only relaxed myocytes isolated from afferent and efferent arterioles as previously described[8] were used in electrophysiological experiments. Myocytes from the rat tail artery (TA) were used as positive control, as both T- and L-type Ca^{2+} currents are consistently reported in these cells (e.g.[16,17]). TA myocytes were dispersed from the tissue with the enzyme solution containing 2mg/ml collagenase NB8, 200U/ml collagenolytic protease, 2mg/ml dispase II and 0.8U/ml elastase III (30-35min, 37ºC). All types of isolated myocytes were studied under identical conditions. Electrophysiological recordings were performed as described previously.[18] Pipettes (resistance 6-12 MΩ) were filled with a solution containing (mmol/L): 120 Cs^+-methansulfonate, 20 CsCl, 5 HEPES, 2 MgATP, 0.5 Na_2GTP, 5 EGTA, 0.3 $MgCl_2$, pH=7.2. The external bath solution contained (mmol/L): 140 NaCl, 5 CsCl, 5 HEPES, 1 $MgCl_2$, 5 glucose, pH=7.35. Ca^{2+} (I_{Ca}) and Ba^{2+} (I_{Ba}) currents were studied in 1.5 mmol/L $CaCl_2$ and 10 mmol/L $BaCl_2$, respectively. Current densities

were calculated by correcting for leak current (off-line) and then dividing by the cell capacitances (C_m).

Current-voltage (*I-V*) relationships for I_{Ca} and I_{Ba} were recorded from a holding potential of -80 mV to activate both the L- and T-type current components. Half-activation voltage (V_a) and the slope factor of activation (k_a) were obtained from normalized whole-cell *I-V*s fitted to the function: $((V_m-E_R)^*g)/(1+\exp((V_m-V_a)/k_a))$, where V_m is membrane potential; E_R the apparent reversal potential and g is the scaling factor. In 35 afferent myocytes, mean E_R and g were 44±2 mV and 0.04±0.004 mV^{-1} (peak I_{Ca}) and 61±1 mV and 0.03±0.002 mV^{-1} (peak I_{Ba}), respectively. In 32 TA myocytes, mean E_R and g were 53±2 mV and 0.06±0.01 mV^{-1} (peak I_{Ca}) and 60±2 mV and 0.02±0.001 mV^{-1} (peak I_{Ba}), respectively.

Ca^{2+} channel availability was investigated by applying 500 ms conditioning voltages (V_C) (between -80 to +40 mV in 10 mV increments) followed by a test pulse (0 or -20 mV). Current amplitudes at the test pulse were normalized and fit to a modified Boltzmann function: $(1-A)/(1+\exp((V_C-V_h)/k_h))$, where V_h and k_h are half-inactivation potential and the slope factor of inactivation, and A is non-inactivating component of the current.

Data are expressed as the means using the standard error of the mean (s.e.m.). Differences between means were evaluated by paired or unpaired Student's *t* test. For multiple measurements, analysis of variance (ANOVA) followed by Bonferroni *post-hoc* test were applied to assess significance. Probabilities with $p<0.05$ were considered significant.

3. Results

At physiologic levels of extracellular Ca^{2+} (1.5 mmol/L), afferent arteriolar myocytes displayed a prominent I_{Ca}. The inward current exhibited a threshold near -30 mV (Fig.1*A* and 1*C*), typical of the L-type Ca^{2+} channels reported in other vascular smooth muscle cells (VSMCs).[19] I_{Ca} reached maximum near 10 mV and had the mean peak amplitude of -8.9±1.3 pA (*n*=36, Fig.1*C*). The properties of these channels were further studied in the presence of extracellular 10 mmol/L Ba^{2+}. It has been previously demonstrated that the L-type I_{Ba} recorded in this concentration of Ba^{2+} is activated in a similar voltage range as I_{Ca} in physiological levels of calcium.[19] Under these conditions, I_{Ba} reached its maximal at 20 mV and mean peak I_{Ba} was increased to 37.1±5.1 pA (*n*=36, Fig.1*B* and 1*C*). The peak I_{Ba} significantly correlated with the size of afferent myocytes expressed as C_m (*p*=0.011). As shown in figure 1*D*, peak I_{Ca} and I_{Ba} densities were -2±0.2 pA/pF and -7.3±0.8 pA/pF, respectively. This ~3.6-fold increase in the current is typical for L-type Ca^{2+} channels.[19,20] In this group of afferent myocytes, C_m ranged from 2.9 to 10.3 pF (mean 5.5±0.3 pF, *n*=36), being similar to 5.6±0.2 pF (range 2.2-11 pF) obtained in 125 myocytes isolated from 87 afferent arterioles and 42 animals.

Notably, no measurable whole-cell inward current was observed in afferent myocytes at membrane potentials negative to -30 mV in either Ba^{2+} or Ca^{2+} (Fig.1*D*). Moreover, the small I_{Ca} and I_{Ba} seen at -20 mV (grey tracings in figures 1*A* and 1*B*) did not exhibit temporal inactivation. Both features are characteristics of the L- and not T-type Ca^{2+} channels. To further pursue this issue, we applied the same approach to myocytes isolated from the rat tail artery (TA), a vessel known to express both the T- and L-type Ca^{2+} channels.[16,17]

Figure 2*A* shows representative I_{Ba} traces recorded from a TA myocyte using the same experimental protocol as shown in Fig.1. Mean *I-V* data comparing I_{Ba} (filled squares) and I_{Ca} (open squares) densities recorded in 32 TA myocytes are depicted in figure 2*B*. Although the general character of *I-V* curves for afferent and TA myocytes were similar, modest differences were discerned. Firstly, the peak I_{Ba} density was significantly larger in the afferent myocytes (-7.3±0.8 pA/pF, n=36) compared to the TA myocytes (-2.7±0.2 pA/pF, n=32, *p*=0.00005), although TA myocytes (C_m=30.9±1.4 pF, *n*=32) were 5.5 times larger than afferent myocytes (C_m=5.5±0.3 pF, *n*=36). Secondly, switching from Ca^{2+} to Ba^{+2} produced a small, albeit significant, shift in the half-activation potential (V_a) of afferent arteriolar myocytes, whereas no such shift was detected in the TA myocytes (Fig.2*C*). Although the V_a for the whole-cell I_{Ba} of TA myocytes (0.8±0.4 mV) was significantly more negative than that of afferent myocytes (3.4±0.5 mV, *p*=0.0003) (Fig.2*C*), the difference was quite modest. Accordingly, the presence of different Ca^{2+} channel types could not be clearly discerned based only on the difference in the activation of the composite whole-cell current as was demonstrated in some VSMCs.[19-21]

In addition to a more negative V_a, T-type Ca^{2+} currents exhibit rapid inactivation which is particularly prominent at negative voltages where the T-component of the current is prevailed over the L-component. The comparison of the representative tracings depicted in grey in figures 1*A* and 2*A* illustrates that I_{Ba} at -20 mV decreases within a 100 ms depolarizing step in the TA myocyte, but not in the afferent myocytes. To highlight this difference in the current kinetics, the mean I_{Ca} and I_{Ba} densities measured at -20 mV in afferent and TA myocytes (leak-corrected off-line) are compared in figures 2*D* and 2*E*, respectively. Both I_{Ca} and I_{Ba} display prominent inactivation in TA myocytes, but not in afferent myocytes.

To further evaluate if the observed difference in the kinetics of I_{Ba} in afferent and TA myocytes represented differing contributions of T- and L-type channels, we used an availability protocol. Figures 3*A* and 3*C* depict traces of I_{Ba} recorded at the test potential of 0 mV following 0.5 s conditioning voltages between -80 and 40 mV for afferent and TA myocytes, respectively. When both L- and T-type Ca^{2+} channels are present, both currents will contribute to the initial peak of the whole-cell I_{Ba}. At the end of 100 ms test pulse, however, the L-type current will dominate, as T-type channels are rapidly inactivated and their contribution to the whole-cell I_{Ba} will thus be diminished (as seen in Fig.*2E*). Moreover, since L- and T-type channels exhibit marked differences in the voltage-dependency of inactivation with the T-type inactivating at more negative voltages than the L-type,[17,19,22] the effects of depolarizing conditioning pulses on the peak I_{Ba} will differ from their effects on I_{Ba} measured at the end of the 100 ms test pulse, if both currents are present. To evaluate this difference in afferent myocytes, the peak I_{Ba} and I_{Ba} measured at the end of 100 ms test pulse were normalized and fitted with a modified Boltzmann function in each cell and the mean values are compared in Figure 3*B*. No significant differences in the half-inactivation potential (V_h), the slope factor of inactivation (k_h) or the non-inactivating component (A) were observed (V_h=-14.6±2.9 mV, k_h=9.2±1.4 mV, A=0.37±0.05 for peak I_{Ba} and V_h=-12.5±2 mV, k_h=8.2±0.9 mV, A=0.35±0.04 for I_{Ba} at 100 ms, n=10). The lack of changes in the voltage-dependent inactivation parameters was also associated with the absence of a substantial effect on I_{Ba} at the test step following by conditioning potentials between -80 and -20 mV (Fig.3*A*, the current at the conditioning potential -20 mV shown in grey).

By contrast, TA myocytes subjected to the same protocol exhibited a significant leftward shift in the availability of the peak I_{Ba} (V_h=-23.1±1.6 mV) compared to that for I_{Ba} at 100 ms (V_h=-10.7±1.1 mV, n=12, p=0.00002, Fig.3*D*). Also, significant changes in k_a (11.4±0.6 mV vs

8.7±0.7 mV, p=0.0033)) and in A (0.25±0.03 vs 0.36±0.03, p=0.00001) for the peak and 100 ms I_{Ba}, respectively, were found. These effects strongly suggest the presence of at least two current components in TA myocytes; with the peak I_{Ba} containing both the T- and L-components whilst I_{Ba} at 100 ms is predominantly the L-type. The similarity between the half-inactivation potential for I_{Ba} at 100 ms in TA myocytes and that for I_{Ba} measured both at the peak and 100 ms in afferent myocytes supports the dominance of the L-type in the latter (compare Fig.3*B* and 3*D*). The analysis of I_{Ba} availability at -20 mV in TA myocytes (Fig.3*D*, filled triangles) where the T-component is dominant, shows even more striking difference with an over 30 mV negative shift in the availability (V_h=-43.4±1.3 mV, k_h=5.6±1.3 mV, A=0.36±0.04, n=9) compared to that for I_{Ba} measured at 100 ms at 0 mV. The size of I_{Ba} at -20 mV in afferent myocytes was too small to derive meaningful availability dependence using this approach.

The presence of the fast inactivating T-type component can also be demonstrated by the analysis illustrated in figure 3*E*. These data depict difference currents obtained by subtracting I_{Ba} at the test potential 0 mV following a conditioning step to -20 mV (when the current is predominantly L-type since the T-type is inactivated as illustrated in Fig.3*D*) from that obtained after a conditioning step to -80 (when both currents are available). As shown in figure 3*E*, a fast-inactivating T-type current is readily demonstrated in the TA myocytes but not in afferent myocytes. The non-inactivating difference current in both cell types is due to the partial inactivation of L-type channels at -20 mV (Fig.3*B* and 3*D*). Furthermore, the analysis of the current kinetics of the mean I_{Ba} densities measured at 500 ms conditioning prepulses to physiologically relevant voltages of -40, -30 and -20 mV in afferent (left) and TA (right) myocytes in figure 3*F* clearly demonstrates fast inactivating kinetics of I_{Ba}, a characteristic property of the T-type current, in TA, but not in afferent, myocytes.

We next examined the effects of nifedipine, a selective L-type Ca^{2+} channel blocker. Figures 4*A* and 4*C* compare the effect of 1 µmol/L nifedipine on the mean I_{Ba} recorded at -20 mV, while figures 4*B* and 4*D* compares the mean *I-V*s in afferent (n=10) and TA (n=13) myocytes. Note that in the afferent myocytes, nifedipine significantly eliminated I_{Ba} inhibiting the current by 75±7% (*p*=0.007). In comparison, in TA myocytes the block of I_{Ba} at -20 mV to nifedipine (Fig.4*C*) was significantly less (27±4%, *p*=0.000005). Moreover, the full *I-V* plot of TA myocytes (Fig.4*D*) revealed a significant blockade at more positive potentials, but clearly exhibited a component of the nifedipine-insensitive voltage-activated inward current. A comparison of the steady-state half-activation parameters disclosed a significant nifedipine-induced leftward shift in V_a in TA myocytes, but not in afferent myocytes (Fig.4*E*). We were able to conduct the availability at 0 mV test potentials in two nifedipine-treated TA myocytes and found V_h to be -38.9 and -37.5 mV, values similar to those seen in the absence of nifedipine at test potentials of -20 mV (Fig.3*D*).

Figure 5 illustrates the effects of 200 nmol/L kurtoxin, a selective inhibitor of T-type Ca^{2+} channels, on afferent (*A*-*D*) and TA (*E*-*H*) myocytes. I_{Ba} was monitored using repeated 100 ms steps from a holding potential of -80 mV to 0 mV, during control periods and following application of kurtoxin. Figures 5*A* and 5*E* depict representative control tracings and tracings obtained after 5 minutes treatment in kurtoxin in the two cell types. In the afferent myocyte kurtoxin caused a small but similar decrease in both the peak and I_{Ba} at 100 ms (Fig.5*A*), whereas in the TA myocyte the inhibitor completely blocked an initial rapidly inactivating component of I_{Ba} but had little effect on I_{Ba} at the end of step depolarization (Fig.5*E*). Figures 5*B* and 5*F* compare the mean kurtoxin-sensitive currents (control minus kurtoxin-treated) and the mean control difference currents (control minus time controls without kurtoxin) in afferent

and TA myocytes, respectively illustrating the effects of kurtoxin and current run-down. Note, that an inactivating, kurtoxin-sensitive current was evident in the myocytes from TA, but not in myocytes from the afferent arteriole. Figures 5*C* and 5*G* depict the time-dependent effects of kurtoxin on the initial peak I_{Ba} in both cell types, whereas figures 5*D* and 5*H* show its effect on the currents measured at 100 ms. To account for run down, data from time controls (*n*=4-5) in which measurements were made in the absence of kurtoxin are depicted as filled symbols in these figures. In TA myocytes, kurtoxin significantly suppressed the peak current by 36.8±6.6% (*p*=0.005, Fig.5*G*), whereas the effect was seen on I_{Ba} at the end of 100 ms was indistinguishable from the time controls (Fig.5*H*). No significant effects of kurtoxin were observed on either peak or 100 ms I_{Ba} in afferent myocytes (Fig.5*C* and 5*D*).

The efferent arteriole is an unusual blood vessel, in that contractile responses are not affected by selective L-type Ca^{2+} channel blockers[4,23] or by hyperpolarization.[11] Similarly, depolarization has no effect on tone or calcium entry in this vessel.[8-10] Conversely, based on responses to non-selective agents that preferentially block T-type channels, it has been suggested that T-type Ca^{2+} channels contribute to the activation of the efferent arteriole.[13,23-25] In this study we were able to obtain the first measurements of I_{Ca} and I_{Ba} in myocytes from isolated efferent arterioles. We could not, however, maintain the whole-cell access long enough statistically compare full *I-V*s in both conditions as in afferent myocytes. Therefore, the whole-cell currents were compared at a test potential to 0 mV. The current traces were leak-subtracted off-line, corrected for the cell size, averaged and compared in Fig.6 with the currents in afferent myocytes recorded under identical conditions. In 1.5 mmol/L Ca^{2+} no measurable inward current was detected in efferent myocytes (Figs.6*A* and 6*B*). With barium as the charge carrier, a small inward current was observed (Fig.6*C*). However, similar to I_{Ca}, it was significantly smaller compared to the afferent myocytes (-0.5±0.4 pA/pF, *n*=5, vs. -

3.5±0.4 pA/pF, n=36)(Fig.6D).   Notably, as in afferent myocytes, the small I_{Ba} seen in efferent myocytes did not display time dependent inactivation (Fig.6C).

4. Discussion

The present study is the first to demonstrate and characterize voltage-activated Ca^{2+} channel currents in myocytes isolated from native afferent and efferent arterioles using direct patch-clamp techniques.   Afferent arteriolar myocytes exhibited a relatively high density of L-type Ca^{2+} currents and these currents could readily be measured in physiologic Ca^{2+}.   By contrast, efferent myocytes did not exhibit a measurable voltage-activated inward current under physiologic Ca^{2+} conditions.   These differences are unlikely due to difference in cell size and different rate of cell dialysis as the cell size (measured as C_m) was similar in both types of arterioles but was 5-fold less than that of TA myocytes which had significantly smaller I_{Ca} and I_{Ba} density then AA myocytes. We could not demonstrate the presence of a measurable T-type Ca^{2+} current in myocytes from either the afferent or efferent arteriole.   These findings support the results of previous studies demonstrating the differing sensitivities of the afferent and efferent arterioles to specific L-type Ca^{2+} channel blocking agents.[3-6,26]

Conversely, our findings do not support the premise that T-type Ca^{2+} channels directly contribute to the activation of either vessel.   A number of laboratories have demonstrated that non-selective T-type channel inhibitors such as mibefradil, efonidipine or pimozide are capable of blocking contractile responses of both afferent and efferent arterioles (see review[13]) and it is suggested that these channels contribute to the activation of both vessels.   It must be emphasized, however, that this premise is supported by indirect observations and relies exclusively on contractile responses.   In contrast, our conclusions are based on the

direct measurements of Ca^{2+} channel currents in single myocytes. Nevertheless, when comparing the results between the intact preparations and enzymatically isolated cells, one could question whether ion channels remain intact in isolated myocytes. To address this possibility, we conducted parallel studies in myocytes isolated from the rat TA using the same cocktail of enzymes. Although the function of the rat tail artery differs from that of the renal arterioles, TA myocytes are the only vascular cell type where the presence of both L- and T-type currents have been consistently documented,[16,17] thus this tissue represented a critical positive control. Another important argument could be that expression of functional Ca^{2+} channels varies between different cells. For example, previous studies found T-type currents only in limited number of VSMCs isolated from the same vessel,[16,17,19] including conduit vessels of the kidney.[21] To address this concern, all myocytes isolated from TA and afferent arterioles and studied with the same protocol were included in our comparative analysis in contrast to previous studies in which exemplary cells expressing either T- or L-type currents were normally compared.

The electrophysiological and pharmacological approaches we used were sufficient to demonstrate the presence of both T- and L-type Ca^{2+} currents in myocytes isolated from the rat tail artery, but not in similarly treated populations of afferent myocytes. Using the key biophysical properties of the T-type Ca^{2+} channels, such as fast inactivating kinetics and more negative voltage range of their activation and inactivation, our analysis clearly demonstrates the presence of all these features in TA myocytes, but not in afferent myocytes (Figures 2-3). The electrophysiological evidence is fully supported by the pharmacological separation of the two type Ca^{2+} currents in TA myocytes using the selective L-type Ca^{2+} channel inhibitor nifedipine and a relatively selective T-type blocker kurtoxin which at 200 nmol/L does not significantly affect the L-type currents[27] (Figures 4-5). Furthermore, a significant leftward

shift in the steady-state activation dependency for I_{Ba} remaining in 1 µmol/L nifedipine in TA, but not in afferent, myocytes (Fig.4*E*) provides further argument against the presence of the T-type currents in the renal afferent myocytes.

Although we did not observe T-type Ca^{2+} currents in these vessels, the expression of the $Ca_V3.1$ and $Ca_V3.2$ genes of the T-type Ca^{2+} channels has been demonstrated in the rat renal afferent arterioles isolated from the superficial regions of the renal cortex or from juxtamedullary nephrons and in the outer medullary vasa recta.[12] We, therefore, cannot rule out the presence of a small, beyond the electrophysiological detection level, T-type current in the afferent arteriole. However, it would be difficult to directly compare protein expression between the two cell types using immunocytochemistry without understanding molecular nature of the T-type Ca^{2+} channels in TA myocytes which has not been established, and is outside the scope of this study. Furthermore, immunocytochemical analysis using antiCa$_V$3.1, antiCa$_V$3.2 and antiCa$_V$3.3 antibodies in vascular SMCs has proven to be inconclusive.[28,29] Functionally, we found that the L-type Ca^{2+} current is rather prominent in afferent arteriolar myocytes with the peak I_{Ca} density measured at physiologic Ca^{2+} was approximately twice that of TA myocytes (Figures 1-2). The size of the current in TA myocytes is comparable to that recorded in other types of arterial myocytes at physiologic levels of Ca^{2+}.[19,30,31] Similarly, the presence of L-type, but absence of detectable T-type Ca^{2+} currents has also been reported in smooth muscle like vasa recta pericytes.[32] Based on our experimental evidence, we therefore suggest that L-type Ca^{2+} channels contribute more importantly to depolarization-induced activation of these vessels. This view is also consistent with the observation that contractile responses and depolarization-induced Ca^{2+} signalling and Ca^{2+} influx of the afferent arteriole are completely blocked by selective L-type antagonists.[4,8,23]

We did not observe a significant voltage-activated inward current in efferent arteriolar myocytes in physiologic Ca^{2+}, although minute I_{Ba} (~7 fold smaller than in afferent myocytes) was detected (Fig.6). This finding is consistent with the lack of effect of potassium-induced depolarization on tone[9,10] and ineffectiveness of selective L-type blockers on this vessel[4] as well as with the lack of their effect on intracellular $[Ca^{2+}]$ or Ca^{2+} influx[8]. Also, no L-type protein was detected in cortical efferent arterioles.[12] One can only speculate on the nature of the Ca^{2+} entry in the efferent arteriole. Previous studies have shown that, unlike the afferent arteriole, angiotensin II-induced vasoconstriction in the efferent arteriole is not dependent on membrane depolarization.[15] Moreover, using the fura-2/manganese quench technique, we have previously shown that angiotensin II activates a voltage-independent and nifedipine-insensitive Ca^{2+} entry in this vessel.[8] The molecular mechanisms and the type(s) of ion channels involved are however not known and require further focused studies.

In the mouse conversely to the rat, Poulsen and co-workers recently reported that potassium-induced depolarization elicits a transient vasoconstriction in isolated efferent arterioles.[7] Since our studies and those cited above were conducted using rat arterioles, the possibility of species differences in the expression of Ca^{2+} channels in the efferent arteriole cannot be ruled out. We also cannot exclude a possibility that afferent and efferent arterioles from juxtamedullary nephrons may express L- and T-type channels in different proportions compared to the superficial cortical arterioles studied in this paper, thus explaining a greater sensitivity of perfused juxtamedullary arterioles to non-specific T-type channel blockers like mibefradil or pimozide.[24] Alternatively, the action of at least some inhibitors may be explained by their action elsewhere due to their lack of specificity via, for example, effects on endothelial channels.[33,34] To our knowledge, the renal microvascular effects of kurtoxin, which is considered to be the most specific T-type Ca^{2+} channel blocker as our study also

suggests, have not been investigated. Accordingly, the possibility that these agents affect the renal microcirculation by actions other than T-type Ca^{2+} channel blockade also merits consideration. A final resolution of this issue awaits further investigations.

Acknowledgements:

Conflict of Interest: None declared.

References

1. Loutzenhiser R, Griffin K, Williamson G, Bidani A. Renal autoregulation: new perspectives regarding the protective and regulatory roles of the underlying mechanisms. *Am J Physiol Regul Integr Comp Physiol* 2006;**290**:R1153-R1167.

2. Packer M, Lee WH, Kessler PD. Preservation of glomerular filtration rate in human heart failure by activation of the renin-angiotensin system. *Circulation* 1986;**74**:766-774.

3. Loutzenhiser R, Epstein M. Effects of calcium antagonists on renal hemodynamics. *Am J Physiol* 1985;**249**:F619-F629.

4. Carmines PK, Navar LG. Disparate effects of Ca channel blockade on afferent and efferent arteriolar responses to ANG II. *Am J Physiol* 1989;**256**:F1015-F1020.

5. Edwards RM, Trizna W, Ohlstein EH. Renal microvascular effects of endothelin. *Am J Physiol* 1990;**259**:F217-F221.

6. Conger JD, Falk SA. KCl and angiotensin responses in isolated rat renal arterioles: effects of diltiazem and low-calcium medium. *Am J Physiol* 1993;**264**:F134-F140.

7. Poulsen CB, Al Mashhadi RH, Cribbs LL, Skøtt O, Hansen PB. T-type voltage-gated calcium channels regulate the tone of mouse efferent arterioles. *Kidney Int* 2011;**79**:443-451.

8. Loutzenhiser K, Loutzenhiser R. Angiotensin II-induced Ca^{2+} influx in renal afferent and efferent arterioles: differing roles of voltage-gated and store-operated Ca^{2+} entry. *Circ Res* 2000;**87**:551-557.

9. Carmines PK, Fowler BC, Bell PD. Segmentally distinct effects of depolarization on intracellular $[Ca^{2+}]$ in renal arterioles. *Am J Physiol* 1993;**265**:F677-F685.

10. Loutzenhiser R, Hayashi K, Epstein M. Divergent effects of KCl-induced depolarization on afferent and efferent arterioles. *Am J Physiol* 1989;**257**:F561-F564.

11. Chilton L, Loutzenhiser K, Morales E, Breaks J, Kargacin GJ, Loutzenhiser R. Inward rectifier K^+ currents and Kir2.1 expression in renal afferent and efferent arterioles. *J Am Soc Nephrol* 2008;**19**:69-76.

12. Hansen PB, Jensen BL, Andreasen D, Skøtt O. Differential expression of T- and L-type voltage-dependent calcium channels in renal resistance vessels. *Circ Res* 2001;**89**:630-638.

13. Hayashi K, Wakino S, Sugano N, Ozawa Y, Homma K, Saruta T. Ca^{2+} channel subtypes and pharmacology in the kidney. *Circ Res* 2007;**100**:342-353.

14. Hayashi K, Homma K, Wakino S, Tokuyama H, Sugano N, Saruta T *et al*. T-type Ca channel blockade as a determinant of kidney protection. *Keio J Med* 2010;**59**:84-95.

15. Loutzenhiser R, Chilton L, Trottier G. Membrane potential measurements in renal afferent and efferent arterioles: actions of angiotensin II. *Am J Physiol* 1997;**273**:F307-F314.

16. Petkov GV, Fusi F, Saponara S, Gagov HS, Sgaragli GP, Boev KK. Characterization of voltage-gated calcium currents in freshly isolated smooth muscle cells from rat tail main artery. *Acta Physiol Scand* 2001;**173**:257-265.

17. Wang R, Karpinski E, Pang PK. Two types of calcium channels in isolated smooth muscle cells from rat tail artery. *Am J Physiol* 1989;**256**:H1361-H1368.

18. Chilton L, Smirnov SV, Loutzenhiser K, Wang X, Loutzenhiser R. Segment-specific differences in the inward rectifier K^+ current along the renal interlobular artery. *Cardiovasc Res* 2011;**92**:169-177.

19. Smirnov SV, Aaronson PI. Ca^{2+} currents in single myocytes from human mesenteric arteries: evidence for a physiological role of L-type channels. *J Physiol* 1992;**457**:455-475.

20. Langton PD, Standen NB. Calcium currents elicited by voltage steps and steady voltages in myocytes isolated from the rat basilar artery. *J Physiol* 1993;**469**:535-548.

21. Gordienko DV, Clausen C, Goligorsky MS. Ionic currents and endothelin signaling in smooth muscle cells from rat renal resistance arteries. *Am J Physiol* 1994;**266**:F325-F341.

22. Loirand G, Mironneau C, Mironneau J, Pacaud P. Two types of calcium currents in single smooth muscle cells from rat portal vein. *J Physiol* 1989;**412**:333-349.

23. Hayashi K, Nagahama T, Oka K, Epstein M, Saruta T. Disparate effects of calcium antagonists on renal microcirculation. *Hypertens Res* 1996;**19**:31-36.

24. Feng MG, Li M, Navar LG. T-type calcium channels in the regulation of afferent and efferent arterioles in rats. *Am J Physiol Renal Physiol* 2004;**286**:F331-F337.

25. Honda M, Hayashi K, Matsuda H, Kubota E, Tokuyama H, Okubo K *et al*. Divergent renal vasodilator action of L- and T-type calcium antagonists *in vivo*. *J Hypertens* 2001;**19**:2031-2037.

26. Takenaka T, Forster H, Epstein M. Protein kinase C and calcium channel activation as determinants of renal vasoconstriction by angiotensin II and endothelin. *Circ Res* 1993;**73**:743-750.

27. Chuang RS, Jaffe H, Cribbs L, Perez-Reyes E, Swartz KJ. Inhibition of T-type voltage-gated calcium channels by a new scorpion toxin. *Nat Neurosci* 1998;**1**:668-674.

28. Kuo IY, Ellis A, Seymour VA, Sandow SL, Hill CE. Dihydropyridine-insensitive calcium currents contribute to function of small cerebral arteries. *J Cereb Blood Flow Metab* 2010;**30**:1226-1239.

29. Nikitina E, Zhang ZD, Kawashima A, Jahromi BS, Bouryi VA, Takahashi M *et al.* Voltage-dependent calcium channels of dog basilar artery. *J Physiol* 2007;**580.2**:523-541.

30. Wang R, Wu Y, Tang G, Wu L, Hanna ST. Altered L-type Ca^{2+} channel currents in vascular smooth muscle cells from experimental diabetic rats. *Am J Physiol Heart Circ Physiol* 2000;**278**:H714-H722.

31. Cox RH, Lozinskaya IM. Ca^{2+} channel inactivation in small mesenteric arteries of WKY and SHR. *Am J Hypertens* 2008;**21**:406-412.

32. Zhang Z, Lin H, Cao C, Khurana S, Pallone TL. Voltage-gated divalent currents in descending vasa recta pericytes. *Am J Physiol Renal Physiol* 2010;**299**:F862-F871.

33. Wu S, Haynes JJ, Taylor JT, Obiako BO, Stubbs JR, Li M *et al.* Cav3.1 (α1G) T-type Ca^{2+} channels mediate vaso-occlusion of sickled erythrocytes in lung microcirculation. *Circ Res* 2003;**93**:346-353.

34. Nilius B, Prenen J, Kamouchi M, Viana F, Voets T, Droogmans G. Inhibition by mibefradil, a novel calcium channel antagonist, of Ca^{2+}- and volume-activated Cl^- channels in macrovascular endothelial cells. *Br J Pharmacol* 1997;**121**:547-555.

Figure Legends:

Figure 1. Calcium channel currents in renal afferent arteriolar myocytes. (**A**) and (**B**) Whole-cell inward currents recorded from a representative cell in the presence of 1.5 mmol/L Ca^{2+} and 10 mmol/L Ba^{2+}, respectively. Traces in grey show currents at -20 mV. C_m=3.1 pF. (**C**) and (**D**) Comparison of *I-V* relationships for the peak (**C**) and the leak-subtracted densities (**D**) for I_{Ca} (○) and I_{Ba} (●), *n*=36.

Figure 2. Comparison of Ca^{2+} channel currents in single renal afferent and TA myocytes. (**A**) I_{Ba} recorded from a representative TA myocyte in 10 mmol/L Ba^{2+}. Trace in grey shows I_{Ba} at -20 mV. C_m=33.1 pF. (**B**) *I-V* relationships for the leak-subtracted peak I_{Ca} (□) and I_{Ba} (■) densities in rat tail arterial myocytes, *n*=32. (**C**) Changes in the mean half-activation potential for I_{Ca} and I_{Ba} in the two cell types (for renal afferent arteriole, *n*=35; for TA, *n*=32; see Methods for further details). (**D**) and (**E**) Comparison of the mean I_{Ca} and I_{Ba}, respectively, recorded at -20 mV in renal afferent arteriolar (*n*=38-39) and TA (*n*=33) myocytes. Currents were leak-corrected off-line, grey lines show s.e.m.

Figure 3. Differences in I_{Ba} inactivation in myocytes from the renal afferent arteriole and tail artery. (**A**) and (**C**) Current traces from a representative renal afferent and TA myocyte, respectively. Traces in grey show current at -20 mV. C_m=30.5 pF. (**B**) and (**D**) Normalized availabilities for the peak I_{Ba} (○,□) and the current at the end of 100 ms test pulse (●,■) in afferent (*n*=10) and TA (*n*=12) myocytes, respectively. Filled triangles show availability for the peak I_{Ba} recorded at the test potential of -20 mV in TA myocytes where the T-type component was predominant (*n*=9). Solid lines are theoretical approximation to the modified Boltzmann equation as described in Methods and in the text. Dashed lines show half-

inactivation potentials. (*E*) Comparison of the mean voltage-sensitive I_{Ba} calculated as the difference current at the test potential 0 mV measured following conditioning potentials to -80 and -20 mV and expressed as current densities. (*F*) Comparison of the mean I_{Ba} densities at negative membrane voltages during a prolonged 500 ms depolarization in the renal afferent arteriolar (left, *n*=10) and TA (right, *n*=12) myocytes.

Figure 4. Effect of the nifedipine on I_{Ba} in renal afferent (*A-B*) and TA (*C-D*) myocytes. (*A*) and (*C*) Mean I_{Ba} density at -20 mV before (Control) and in the presence of 1 µmol/L nifedipine in afferent (*n*=10) and TA (*n*=13) myocytes, respectively. (*B*) and (*D*) Normali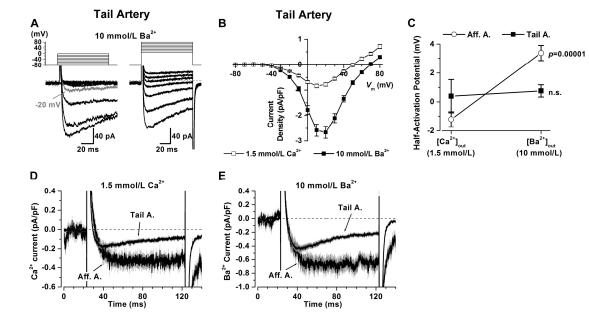zed *I-V* in the absence (open symbols) and presence (closed symbols) of nifedipine. (*E*) Diverge effect of nifedipine on the Ca^{2+} channel activation in TA (*n*=13) and renal afferent (*n*=7; in 3 cells I_{Ba} in the presence of nifedipine was too small to be theoretically approximated) myocytes.

Figure 5. Comparison of the effect of the T-type Ca^{2+} channel inhibitor kurtoxin on I_{Ba} in renal afferent (*A-D*) and tail arterial (*E-H*) myocytes. (*A*) and (*E*) I_{Ba} at 0 mV before (Control) and 5 min after addition of 200 nmol/L kurtoxin in a representative renal afferent arteriolar (C_m=4.5 pF) and tail arterial (C_m=38.6 pF) myocyte, respectively. (*B*) and (*F*) Mean kurtoxin-sensitive I_{Ba} (derived as a difference between I_{Ba} before and 5 min after addition of kurtoxin in each cell, *n*=5 for both cell types) and mean control difference I_{Ba} (calculated at the same time points as for kurtoxin but in the absence of the blocker in 4 afferent and 6 tail arterial myocytes), respectively. Grey lines show s.e.m. (*C-D*) and (*G-H*) Comparison of the time-dependence of the current block measured at the peak (10-12 ms, *C* and *G*) and at the end of 100 ms (*D* and *H*) voltage step to 0 mV. Kurtoxin was applied at time 0 for 5 min (filled symbols). Open symbols show time control run in the absence of the inhibitor, *n*=4-6.

Figure 6. Calcium channel currents in rat renal efferent arterioles. (***A***) and (***C***) Comparison of the mean I_{Ca} and I_{Ba} densities recorded at 0 mV in myocytes isolated from efferent and afferent arterioles as indicated. Grey lines show s.e.m. (***B***) and (***D***) Statistical comparison of the peak densities for I_{Ca} and I_{Ba}, respectively, in the efferent and afferent myocytes.

Afferent Arteriole

A Tail Artery
(mV)
10 mmol/L Ba²⁺
-20 mV
40 pA
20 ms
40 pA
20 ms

B Tail Artery
Current Density (pA/pF)
V_m (mV)
□ 1.5 mmol/L Ca²⁺   ■ 10 mmol/L Ba²⁺

C
○ Aff. A.   ■ Tail A.
Half-Activation Potential (mV)
p=0.00001
n.s.
[Ca²⁺]out (1.5 mmol/L)   [Ba²⁺]out (10 mmol/L)

D 1.5 mmol/L Ca²⁺
Ca²⁺ current (pA/pF)
Tail A.
Aff. A.
Time (ms)

E 10 mmol/L Ba²⁺
Ba²⁺ Current (pA/pF)
Tail A.
Aff. A.
Time (ms)

Afferent Arteriole

Tail Artery

A

0.5 s   0 mV   0.5 s

40
0
-40
-80

-20 mV

20 pA
200 ms

20 pA
200 ms

C

0.5 s   0 mV   0.5 s

40
0
-40
-80

-20 mV

30 pA
200 ms

30 pA
200 ms

E

I_{Ba} (pA/pF)

0
-1
-2

Tail A.

Aff. A.

610   640   680   720
Time (ms)

B

Normalized I_{Ba}

1.0
0.5
0.0

V_t= 0 mV
○ Peak
● End 100 ms

-80 -60 -40 -20 0 20 40
Conditioning Potential (mV)

D

Normalized I_{Ba}

1.0
0.5
0.0

V_t= 0 mV
□ Peak
■ End 100 ms
V_t=-20 mV
▲ Peak

-80 -60 -40 -20 0 20 40
Conditioning Potential (mV)

F

Aff.A.   Tail A.

I_{Ba} (pA/pF)
0.4
0.0
-0.4

-40 mV   -40 mV

I_{Ba} (pA/pF)
0.4
0.0
-0.4

-30 mV   -30 mV

I_{Ba} (pA/pF)
0.4
0.0
-0.4
-0.8
-1.2

-20 mV   -20 mV

200 400 600   200 400 600
Time (ms)   Time (ms)

Afferent Arteriole

A

$V_m = -20$ mV

Nifedipine

Control

I_{Ba} (pA/pF)

Time (ms)

B

Normalized I_{Ba}

V_m (mV)

○— Control ●— 1 μmol/L Nifedipine

Tail Artery

C

$V_m = -20$ mV

Nifedipine

Control

I_{Ba} (pA/pF)

Time (ms)

D

Normalized $I_{Ba(Peak)}$

V_m (mV)

□— Control ■— 1 μmol/L Nifedipine

E

○ Aff.A. ■ Tail.A.

Half-Activation Potential (mV)

n.s.

$p=0.0012$

Control   Nifedipine

Afferent Arteriole

A
B
C
D

Tail Artery

E
F
G
H